

ARTICLE OPEN



A real-world clinical validation for AI-based MRI monitoring in multiple sclerosis

Michael Barnett^{1,2,3,16}, Dongang Wang^{1,2,16}, Heidi Beadnall^{2,3}, Antje Bischof⁴, David Brunacci⁵, Helmut Butzkueven^{6,7}, J. William L. Brown⁸, Mariano Cabezas², Tilak Das⁹, Tej Dugal^{1,10}, Daniel Guilfoyle³, Alexander Klistorner^{1,2,11}, Stephen Krieger¹², Kain Kyle^{1,2}, Linda Ly¹, Lynette Masters¹³, Andy Shieh¹, Zihao Tang^{1,2}, Anneke van der Walt^{5,6}, Kayla Ward^{1,2}, Heinz Wiendl⁴, Geng Zhan^{1,2}, Robert Zivadinov¹⁴, Yael Barnett^{1,15,17} and Chenyu Wang^{1,2,17}✉

Modern management of MS targets No Evidence of Disease Activity (NEDA): no clinical relapses, no magnetic resonance imaging (MRI) disease activity and no disability worsening. While MRI is the principal tool available to neurologists for monitoring clinically silent MS disease activity and, where appropriate, escalating treatment, standard radiology reports are qualitative and may be insensitive to the development of new or enlarging lesions. Existing quantitative neuroimaging tools lack adequate clinical validation. In 397 multi-center MRI scan pairs acquired in routine practice, we demonstrate superior case-level sensitivity of a clinically integrated AI-based tool over standard radiology reports (93.3% vs 58.3%), relative to a consensus ground truth, with minimal loss of specificity. We also demonstrate equivalence of the AI-tool with a core clinical trial imaging lab for lesion activity and quantitative brain volumetric measures, including percentage brain volume loss (PBVC), an accepted biomarker of neurodegeneration in MS (mean PBVC -0.32% vs -0.36% , respectively), whereas even severe atrophy ($>0.8\%$ loss) was not appreciated in radiology reports. Finally, the AI-tool additionally embeds a clinically meaningful, experiential comparator that returns a relevant MS patient centile for lesion burden, revealing, in our cohort, inconsistencies in qualitative descriptors used in radiology reports. AI-based image quantitation enhances the accuracy of, and value-adds to, qualitative radiology reporting. Scaled deployment of these tools will open a path to precision management for patients with MS.

npj Digital Medicine (2023)6:196; <https://doi.org/10.1038/s41746-023-00940-6>

INTRODUCTION

Multiple sclerosis (MS) is the most common inflammatory demyelinating and neurodegenerative condition of the central nervous system, afflicting some 2.8 million persons globally¹. Characterized by both focal lesions and by more diffuse neurodegeneration in the brain and spinal cord, MS results in significant physical and cognitive disability and, in many cases, premature withdrawal from the workforce.

Highly effective disease-modifying therapy (DMT) dramatically reduces the risk of relapse associated worsening (RAW), but has limited impact on progression independent of relapse activity (PIRA), the principal driver of increasing disability in patients with established, treated disease^{2–4}. Inflammatory activity, the pathological substrate for RAW, and response to DMT are monitored by regular clinical assessment and repeated magnetic resonance imaging (MRI), usually on an annual basis⁵. MRI is also the most important tool for neurologists to assess disease activity that does not manifest with overt clinical change, but potentially injures vast numbers of axons and disrupts complex integrated brain networks. Specifically, the development of new or enlarging hyperintensities on FLAIR MRI and/or new contrast-enhancing lesions (CELs) on T1-w MRI generally suggests inadequate suppression of inflammatory activity and may prompt the clinician

to change the patient's DMT⁵. PIRA is more difficult to characterize by MRI, but at the group level disability worsening correlates well with whole brain volume change^{6,7}. In the absence of available DMTs that specifically target neurodegeneration, MRI evidence of accelerated brain atrophy, which at the individual level can be confounded by biological, disease- and treatment-related fluctuations, is generally not used in isolation to drive treatment change. However, there is broad agreement that the modern management of MS should target "NEDA-3", or No Evidence of Disease Activity (no clinical relapses, no MRI activity, no disability worsening)⁸.

The radiologist therefore plays a critical role, not only in the diagnosis of MS, but in the monitoring of the disease and its response to DMT. Traditionally, detailed slice-by-slice examination of current and prior study FLAIR images is required to accurately exclude the development of new or enlarging lesions, a painstaking process that has become increasingly burdensome with the advent of 3D imaging, which generates up to 300 slices in a single volume. Lack of current and prior 3D FLAIR volume co-registration in many picture archiving and communications systems (PACS) can also hamper the accurate detection of small new lesions or minor lesion enlargement, particularly when concentric, between studies. While the volume of new (or enlarging) lesions may impact treatment strategy, this is not

¹Sydney Neuroimaging Analysis Centre, Sydney, NSW, Australia. ²Brain and Mind Centre, University of Sydney, Sydney, NSW, Australia. ³Department of Neurology, Royal Prince Alfred Hospital, Camperdown, NSW, Australia. ⁴Department of Neurology, University Hospital of Muenster, Muenster, Germany. ⁵Department of Radiology, Royal Prince Alfred Hospital, Camperdown, NSW, Australia. ⁶Department of Neurology, The Alfred Hospital, Melbourne, VIC, Australia. ⁷Department of Neuroscience, Central Clinical School, Monash University, Melbourne, VIC, Australia. ⁸Department of Clinical Neurosciences, University of Cambridge, Cambridge, UK. ⁹Department of Radiology, University of Cambridge, Cambridge, UK. ¹⁰Synergy Radiology, Sydney, NSW, Australia. ¹¹Save Sight Institute, University of Sydney, Sydney, NSW, Australia. ¹²Department of Neurology, Icahn School of Medicine at Mount Sinai, New York, NY, USA. ¹³MED Radiology, Sydney, NSW, Australia. ¹⁴Buffalo Neuroimaging Analysis Centre, Buffalo, NY, USA. ¹⁵Department of Radiology, St Vincent's Hospital, Sydney, NSW, Australia. ¹⁶These authors contributed equally: Michael Barnett, Dongang Wang. ¹⁷These authors jointly supervised this work: Yael Barnett, Chenyu Wang. ✉email: tim@snacc.com.au

Table 1. iQ-Solutions™ MS Report output: metrics^a.

Cross-sectional metrics	Longitudinal changes from previous scan
FLAIR lesion number and volume	Longitudinal protocol warnings (T1 and FLAIR) ^c
FLAIR lesion volume patient ^b centile	New FLAIR lesion number and volume
T1-w contrast enhancing lesion number and volume	Enlarging FLAIR lesion number and volume
Normalized whole brain volume	Annualized percentage brain volume change
Normalized whole brain volume centile ^{a,d}	
Normalized thalamus volume	
Normalized thalamus volume HC centile ^d	

^aiQ-MS experiential MS reference dataset only available in the tool's research mode.
^bCompared with iQ-MS underlying MS reference dataset.
^cProvided in research mode when scanner/protocol inconsistencies detected (Supplementary data).
^dCompared with iQ-MS underlying healthy control dataset.

measured or reported in routine clinical radiology practice. An estimation of the severity of the overall FLAIR lesion burden, which provides prognostic information, is also dependent on the experience of the reporting radiologist and can only be semi-quantitatively assessed. Severe brain volume loss (BVL) versus age-matched healthy controls, which may also be of prognostic significance, can be detected by experienced radiologists with visual inspection but cannot be accurately quantitated without additional tools, which are generally confined to research settings. Moderate changes (of the magnitude expected in many patients with MS) are difficult, if not impossible, to recognize by visual inspection alone^{9,10}. Similarly, longitudinal change in brain volume during the typical 12-month interval between MRI scans is usually small and not detectable by visual inspection. While short-term changes in brain volume are difficult to interpret in individual patients, a consistent adverse trajectory over multiple clinical epochs or more severe brain atrophy (>0.8% percent BVL per annum) over a single epoch, may influence or support clinical decisions to escalate or switch DMT⁵.

Recognition that clinical radiology reports for patients with MS can be enhanced by quantitative information has been accompanied, in the last 5 years, by the development of artificial intelligence (AI) algorithms for medical imaging that can automate both the detection and segmentation of the brain, brain substructures and different types of brain pathology, including MS lesions^{11–14}. While there are a small number of existing commercial (regulatory-approved) image analysis tools that have been designed to assist radiologists and clinicians who treat patients with MS, thorough real-world clinical validation is limited¹⁵. Here, we report a comprehensive clinical evaluation of iQ-Solutions™ (MS Report), hereafter referred to as iQ-MS, in a large cohort of MS scan pairs that were independently reported in clinical practice by expert radiologists; and, separately, were quantitatively and blindly assessed by trained neuroimaging analysts in a core reading imaging laboratory using standard procedures (SOPs) used in regulatory trials. Specifically, we hypothesized that the AI tool would more sensitively and accurately detect MRI evidence of disease activity compared with conventional radiology reports; and produce cross-sectional and longitudinal brain volumetric measurements comparable with those generated by conventional imaging tools implemented by the core lab.

iQ-Solutions™ analyses brain MRI scans in Digital Imaging and Communications in Medicine (DICOM) format using a collection of AI algorithms based on deep neural network technology, and was developed using more than 8500 brain scans that had been expertly annotated by trained neuroimaging analysts. iQ-Solutions™ produces an MS-specific report that includes cross-sectional and longitudinal whole brain, brain substructure and

lesion metrics relevant to the condition (Table 1). The AI tool returns visualizations of relevant segmentations to the PACS for radiologist review (Fig. 1).

For any analysis to proceed, images are automatically quality-checked to ensure that pre-contrast 3D-T1 and 3D FLAIR sequences, each containing ≥ 30 slices with a thickness of ≤ 3 mm, are available. All cross-sectional segmentation algorithms (Table 1) were developed with 3D-UNet¹⁶ as the core network for extracting image features, followed by a solitary convolutional layer as the prediction head. Cross-validation was conducted through comparison (based on case-wise and voxel-wise DICE scores) with ground-truth masks produced by trained neuroimaging analysts. Similarly, lesion activity between timepoints (namely, the development of new and enlarging lesions) is measured by iQ-Solutions using an algorithm based on a modified 3D-Unet and trained with manually annotated 3D-FLAIR images, as described previously¹⁷. iQ-MS reports enlarging lesions as new lesional voxels that are connected to an existing lesion (on the prior study) within its 26-voxel neighbourhood.

For brain and substructure volumetric analyses, a lesion-inpainting model, LG-Net, was applied to 3DT1 images to ameliorate segmentation bias generated by the presence of MS lesions, as previously described¹⁸. For longitudinal brain and brain substructure volumetric change, iQ-Solutions performs a number of checks for image consistency between the two scan timepoints (Supplementary Method). Longitudinal metrics are reported, but returned to the user with a protocol inconsistency warning. Longitudinal whole brain volume change is measured by iQ-MS with the integrated DeepBVC algorithm¹⁹. Automated estimation of substructure (whole gray matter, thalamus) volume change is produced by a combination of AI-based segmentation and the application of a Jacobian integration method²⁰.

iQ-MS presents volumetric data for individual patients as normalized values; and as centiles referenced to a hypothetical age-matched healthy control. iQ-MS additionally reports brain volumetrics and MS lesion volumes benchmarked to a hypothetical person with MS of similar age, disease duration and disability, to provide a more clinically meaningful, experiential reference. Reference cohorts were created using MRI scans from more than 3000 healthy controls and an independent sample of 839 people with MS, analyzed with the same methods.

RESULTS

Study demographics

Of 400 unique scan pairs included in the study, three failed iQ-MS processing due to missing slices in the 3D FLAIR sequence ($n = 2$) or unknown technical reasons ($n = 1$) and were excluded from further analysis. The remaining 397 scan pairs were acquired with

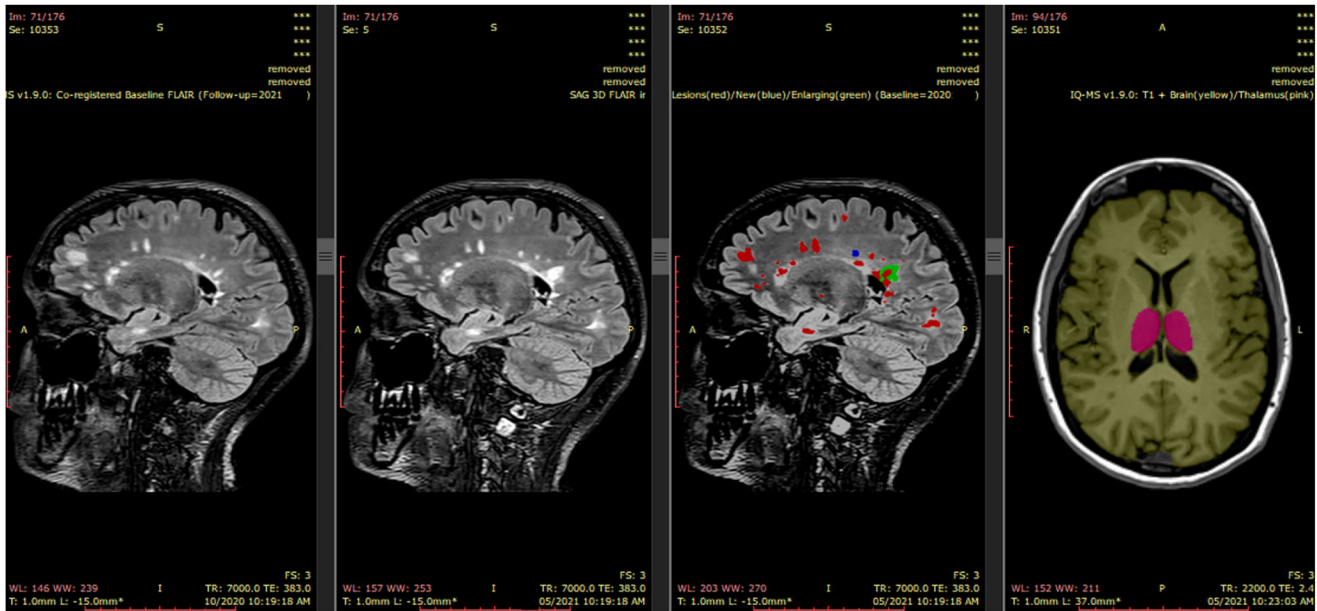


Fig. 1 iQ-Solutions™ PACS integration. iQ-MS automatically returns a co-registered baseline (prior study) 3D FLAIR series together with a lesion-annotated 3D FLAIR, here showing a case with both new (blue) and enlarging (green) lesions. A 3D-T1 series is also returned with both whole brain (yellow) and thalamus (pink) annotations. From left to right images : Co-registered FLAIR from patient’s last scan; FLAIR image of the current MRI exam; Lesion masks overlaid on current FLAIR image; Brain and Thalamus masks overlaid on current 3DT1 image.

Table 2. Distinct incidental findings on MS clinical radiology reports.

Incidental finding	Number of Scans (%)
Meningioma	8 (2)
Stroke	4 (1)
Focal gliosis	4 (1)
Cavernoma	3 (0.8)
Vestibular schwannoma	2 (0.5)
Nasolabial cyst	2 (0.5)
Intrasellar lesion	2 (0.5)
Developmental venous anomaly	2 (0.5)
Arteriovenous malformation	2 (0.5)
Pineal cyst	1 (0.3)
Neuroglial cyst	1 (0.3)
Left parotid lesion	1 (0.3)
Focal hyperostosis	1 (0.3)
Dural calcification	1 (0.3)
Dilated perivascular space	1 (0.3)
Cryptococcoma	1 (0.3)
Cortical dysplasia	1 (0.3)
Choroid plexus cyst	1 (0.3)
Cerebral artery aneurysm	1 (0.3)
Cerebellar ectopia	1 (0.3)
Cerebral contusion	1 (0.3)
Arachnoid cyst	1 (0.3)
Total	42 (10.6)

a mean interval 12 months (range 6–29 months) from 282 unique patients (F:M = 198:84) with a disease duration of 13.1 years (range 0.71–41.83 years) and median EDSS was 1.5 (range 0–7.0, n = 315) at the time of the study (follow-up) scan (see

Supplementary Table 1 for details). Incidental findings were present (as determined by the radiology report) in 10.6% of study scans (n = 397, Table 2). The vast majority of study scans (387/397) were performed on one of three scanners, each located in different MRI centers: GE MR750 3T (GE Healthcare, Milwaukee, USA) (n = 174), Philips Ingenia 3 T (Philips Inc, Amsterdam, The Netherlands) (n = 159) and Siemens Skyra 3T (SIEMENS Healthineers, Erlangen, Germany) (n = 54). 318/397 scan pairs were acquired on the same scanner with a longitudinally stable protocol defined by iQ-MS (Supplementary methods). The scan workflow for inclusion of scans for all analyses is illustrated in Supplementary Fig. 1.

Lesion metrics. Total FLAIR lesion volume determined by iQ-MS was automatically converted to a centile against an (independent) MS patient population built into the tool, and compared against a numerical rating scale/centile assigned to categorical variables in the clinical radiology report, as shown in Table 3. Lesion burden, described in the radiology report of 267/397 unique study (follow-up) scans, matched the equivalent iQ-MS centile in 183/267 (68.5%) of scans; of the remaining scans, the iQ-MS lesion burden fell in a higher centile range in 69/84 (82.1%) of cases. There was a high correlation for both mean FLAIR lesion number (iQ-Solutions: 47.8 [SD 39.0], range 0–223; core lab: 56.0 [SD 44.7], range 1–269; $R^2 = 0.96, p < 0.001$) and volume (iQ-Solutions: 6.4 mls [SD 10.3], range 0–66.7; core lab: 7.9 mls [SD 11.0], range 0–73.1, $R^2 = 0.96, p < 0.001$) as detected by iQ-Solutions and the core reading lab. The FLAIR lesion burden also correlated moderately with normalized brain volume (NBV) generated by both iQ-MS ($R^2 = 0.31, p < 0.001$) and the core reading laboratory ($R^2 = 0.24, p < 0.001$). Disability, as measured by EDSS, correlated only weakly with cerebral FLAIR lesion burden as determined by both methods ($R^2 = 0.16, p < 0.001$ and $R^2 = 0.15, p < 0.001$ respectively), though significance of the correlation persisted after correction for age, sex, disease duration, and brain volume.

Table 4 shows the number of scan pairs in which new/enlarging FLAIR lesions or CELs were identified; and the mean new and enlarging lesion numbers for each of the three analysis methods,

Table 3. Clinical radiology report FLAIR lesion burden descriptors.

Clinical descriptor	Numerical assignment	Final assignment	Equivalent iQMS™ Burden (patient ^a centile)
• No cerebral lesions	0	Mild	<25%
• Single lesion	1		
• Very scant	2		
• Very mild, scant	3		
• Relatively scant, mild, relatively mild, small, few, a few, several	4		
• Mild to moderate	5	Moderate	25–75%
• Moderate	6		
• Moderately extensive, significant, moderate to heavy, moderate to marked, numerous	7	Severe	>75%
• Extensive, Severe	8		

^aCompared with iQ-MS underlying MS reference dataset.

and for the expert consensus. In total, case-level discrepant results were found in 53/397 case pairs for the presence of new and enlarging lesions; and in 10/180 cases for the presence of CELs. At the lesion number level, discrepancies were present in 51/397 cases (new lesions), 57/397 cases (enlarging lesions), 13/180 cases (CELs), 74/397 cases (new or enlarging lesions), and 78/397 cases (new or enlarging lesions or CELs) among any of the three analysis methods. The outputs and relevant segmentations of all 78 cases exhibiting any discrepancy were manually reviewed (MB, YB) to develop the expert consensus. Visual analysis of twenty randomly selected case-level discrepant pairs (and their analysis outputs) by an independent expert neuro-radiologist (DB), blinded to the expert consensus, corroborated the results of the expert consensus in all cases.

Using the expert consensus as ground truth, iQ-MS more sensitively detected new or enlarging FLAIR (93.3%) lesions and T1-w CELs (85.7%) than either the radiology report (58.3% and 57.1%, respectively) or core MRI reading lab (85.0% and 71.4%, respectively). When the analysis was restricted to scan pairs with a longitudinally stable scanner/protocol (see Supplementary methods, $n = 318$), iQ-Solutions and the core MRI reading center detected new/enlarging lesions with equivalent sensitivity (91.7%), and there was a modest improvement in the sensitivity of the radiology report (60%). Specificity for the detection of FLAIR new/enlarging and T1-w CELs were high for iQ-MS (97.6%, 97.1%, respectively), the radiology report (98.8%, 98.8% respectively) and the core MRI reading lab (96.4%, 99.4%); and improved even further when analysis was restricted to scan pairs with a longitudinally stable scanner/protocol (Table 4). For a subset of scans reported by fellowship-trained neuroradiologists ($n = 268$), iQ-MS, radiology reports and the core lab detected MS disease activity in longitudinally stable scans with a sensitivity of 91.0%, 76.0%, and 87.9%.

At the lesion level, iQ-Solutions failed to detect an average of 0.02 new lesions per scan using the expert consensus as the gold standard, whereas the core lab and radiology reports failed to detect an average of 0.05 and 0.07 new lesions per scan, respectively. For enlarging lesions, the average number of missed lesions per scan for the three techniques was 0.02, 0.09, and 0.16 respectively.

Brain volumetrics. Of the 397 cross-sectional study scans analyzed for brain volume by iQ-MS, 36 cases failed quality control imposed by the core reading lab's SOP (Supplementary methods) and were deemed unsuitable for analysis by SIENAX. Comparisons between the methods were therefore restricted to remaining 361 cases. Mean cross-sectional brain volume, reported by iQ-MS and the core MRI reading lab (using SIENAX) are shown in Table 5, together with relevant healthy control centile data. NBV was considered to be within normal limits at or above the healthy control 25th centile for

both iQ-MS and SIENAX. NBV below this cut-off were identified by these tools in 54.3% and 74.9% of scans respectively; and more severe brain volume loss (≤ 10 th centile) was identified in 32.5% and 38.5% of patients respectively. NBV derived from SIENAX exhibited a greater degree of variance than iQ-MS. Despite these differences, there was a good correlation between NBV derived by the two tools ($R^2 = 0.671$, $p < 0.001$); and NBV correlated, albeit relatively weakly, with EDSS for both (iQ-MS $R^2 = 0.23$, $p < 0.001$; SIENAX $R^2 = 0.14$, $p < 0.001$). Similar observations were made for normalized gray matter and thalamic volumes measured by both iQ-MS and the core MRI reading lab's implementation of FIRST (Table 5). In a univariate general linear model including NBV, normalized thalamic volume, lesion volume and sex, only NBV ($p < 0.001$) and normalized thalamic volume ($p = 0.012$) were significant contributors to the overall model's power to predict EDSS ($R^2 = 0.28$, $p < 0.001$). However, the addition of age substantially improved the model's power ($R^2 = 0.35$, $p < 0.001$) and rendered the contribution of NBV non-significant ($p = 0.352$), while preserving the significance of normalized thalamic volume ($p < 0.001$) as a significant predictor of EDSS, in keeping with the known association of this structure with MS disease progression²¹. An analogous pattern was observed using metrics derived from the core lab. Notably, radiology reports only described the presence or absence of brain volume loss in 99/397 study scans, of which 23% were reported to have some degree of brain volume loss, though this was not categorized in vast majority, preventing meaningful statistical comparison. None of the radiology reports described thalamic volume change.

Mean interval brain atrophy was calculated for all pairs that passed longitudinal analysis criteria defined by the iQ-Solutions automated protocol QC/analysis ($n = 318$, see Supplementary methods for details). Of these pairs, a further 23 failed quality control imposed by the core reading lab's relevant SOP (see Supplementary methods for details) and were deemed unsuitable for analysis by SIENAX. Comparisons between the methods were therefore restricted to remaining 295 scan pairs. Mean annualized PBVC was similar for both methods (iQ-MS: -0.32% [SD -0.73%]; SIENAX: -0.36% [SD -0.71%]). There was a strong correlation ($R^2 = 0.86$, $p < 0.001$) between annualized PBVC determined by the two methods (Fig. 2). Using a pathological cut-off of 0.4% PBVC²², brain atrophy was detected in 134/295 (45.4%) of study scans using both quantitative methods; and severe brain atrophy ($>0.8\%$ per year) was also equivalently detected in 64/295 (21.7%) of scans. However, at the individual scan level, classification of annualized atrophy as severe ($>0.8\%$) was discordant in 24/295 cases. Of these cases, a difference of more than 0.2% was observed in 15/24 between iQ-Solutions (greater atrophy in eight patients) and SIENAX (greater atrophy in seven patients). Qualitative assessment of brain

Table 4. Comparison of lesion metrics.

	iQ-Solutions™	Core MRI Lab	Radiology Report	Consensus Review	<i>n</i>
Mean FLAIR Lesion Number [SD], Range	47.8 [39], 0–223	56.0 [44.7], 1–269	—	—	397
Mean FLAIR Lesion Volume [SD], Range	6.4 [10.3], 0–66.7	7.9 [11.0], 0–73.1	—	—	
Lesion Number Correlation	$R^2 = 0.964$, $p < 0.001$		—	—	
Lesion Volume Correlation	$R^2 = 0.962$, $P < 0.001$		—	—	
Cases with New or Enlarging Lesions (all stable protocol*)	64 50	63 51	39 31	60 48	397 318
Mean New Lesion number (all stable protocol)	0.24 0.22	0.17 0.19	0.18 0.20	0.20 0.22	
Mean Enlarging Lesion number (all stable protocol)	0.36 0.33	0.17 0.16	0.05 0.04	0.20 0.20	
Sensitivity: New and Enlarging Lesions (all stable protocol)	<u>93.3</u> <u>91.7</u>	85.0 <u>91.7</u>	58.3 60.4	—	
Specificity: New and Enlarging Lesions (all stable protocol)	97.6 <u>97.8</u>	96.4 <u>97.4</u>	<u>98.8</u> <u>99.3</u>	—	
Accuracy: New and Enlarging Lesions (all stable protocol)	<u>0.97</u> <u>0.97</u>	0.95 <u>0.97</u>	0.93 <u>0.93</u>	—	
Precision: New and Enlarging Lesions (all stable protocol)	0.88 <u>0.88</u>	0.81 <u>0.86</u>	<u>0.90</u> <u>0.94</u>	—	
F1 score: New and Enlarging Lesions (all stable protocol)	<u>0.90</u> <u>0.90</u>	0.83 <u>0.89</u>	0.71 <u>0.73</u>	—	
Mean New/Enlarging Lesion Volume (ml) [SD], Range (all)	0.04 [0.24], 0–3.05	—	—	—	397
Study Scans with Gd+ Lesions	11	6	6	7	180
Mean Gd+ Lesion Number	0.09 [0.39], 0–3.00	0.038889	0.06	0.056738	
Sensitivity: Gd+ Lesions	<u>85.7</u>	71.4	57.1	—	
Specificity: Gd+ Lesions	<u>97.1</u>	<u>99.4</u>	98.8	—	
Mean Gd+ Lesion Volume (ml) [SD], Range	0 [0.02], 0–0.19	0 [0.01], 0–0.13	—	—	

Table 5. Comparison of brain volumetrics.

	iQ-Solutions™	Core MRI Lab	Radiology Report
Cross-sectional volumetrics, <i>n</i> = 361 unique scan pairs			
Mean Normalized* Brain Volume [SD] (ml)	1460.4 [56.2]	1427.4 [77.0]	—
Mean Normalized Thalamic Volume [SD] (ml)	18.2 [2.1]	19.2 [2.2]	—
Mean Normalized Gray Matter Volume [SD] (ml)	772.3 [38.3]	755.5 [48.9]	—
NBV HC Centile® (%), ≥25th	44.9	13.0	19.1 (“No BVL”)
NBV HC Centile® (%), 10th–25th	20.2	27.4	5.8 (“BVL”)
NBV HC Centile® (%), ≤10th	34.9	59.6	75.1 (Unknown)
Normalized Brain Volume Correlation	$R^2 = 0.67$, $p < 0.001$		—
Normalized Thalamic Volume Correlation	$R^2 = 0.80$, $p < 0.001$		—
Normalized Gray Matter Volume Correlation	$R^2 = 0.69$, $p < 0.001$		—
Longitudinal volumetrics, <i>n</i> = 295 unique scan pairs			
Mean Interval PBVC Change [SD] (%)	−0.32 [−0.73]	−0.36 [−0.71]	—
PBVC Correlation	$R^2 = 0.86$, $p < 0.001$		—
Interval PBVC Severity (Loss) <i>n</i> (%), < 0.4%	161 (54.6%)	161 (54.6%)	80% (“No atrophy”)
Interval PBVC Severity (Loss) <i>n</i> (%), 0.4–0.8%	70 (23.7%)	70 (23.7%)	20% (Unknown)
Interval PBVC Severity (Loss) <i>n</i> (%), >0.8%	64 (21.7%)	64 (21.7%)	
Interval Thalamic Volume Change [SD] (%)	−0.33 [1.75]	—	—
Interval Gray Matter Volume Change [SD] (%)	−0.15 [1.02]	—	—

NBV normalized brain volume, PBVC percent brain volume change.

volume change in scan pairs was described in 236/295 radiology reports; no interval atrophy was reported in any of the assessed scan pairs.

Interval iQ-MS PBVC was weakly correlated with both new ($R = -0.11$, $p < 0.05$) and enlarging ($R = -0.13$, $p < 0.01$) lesion

volume; and survived partial correlation correction for age, sex and disease duration. SIENA-derived PBVC was not correlated with any of these variables. There was also a weak correlation of PBVC, as derived by both methods, with EDSS that survived correction for age, sex and disease duration (Table 6).

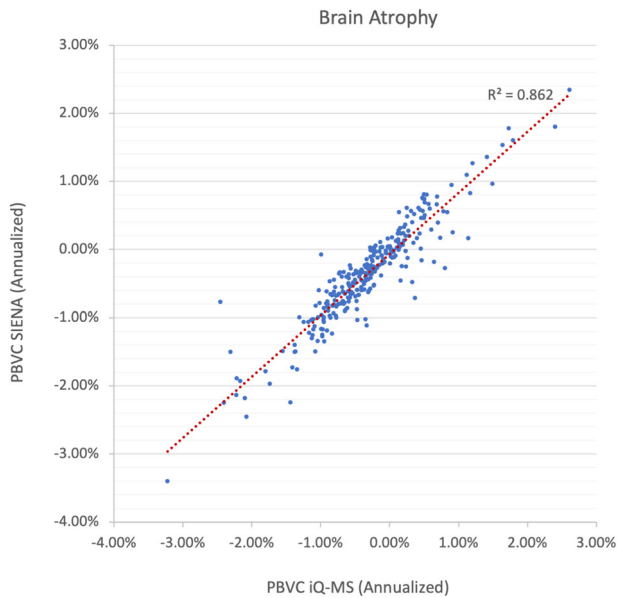


Fig. 2 Correlation of annualized percentage brain volume change between scan pairs as determined by SIENA and iQ-MS. PBVC percentage brain volume change.

	iQ-Solutions™	Core MRI Lab
NBV-EDSS	$R^2 = 0.23, p < 0.001$	$R^2 = 0.14, p < 0.001$
NTV-EDSS	$R^2 = 0.21, p < 0.001$	$R^2 = 0.17, p < 0.001$
GMV-EDSS	$R^2 = 0.23, p < 0.001$	$R^2 = 0.12, p < 0.001$
PBVC-EDSS	$R^2 = 0.05, p < 0.001$	$R^2 = 0.03, p = 0.04$
Lesion Volume-EDSS	$R^2 = 0.16, p < 0.001$	$R^2 = 0.15, p < 0.001$
New Lesion Volume-EDSS	Not significant	—
Enlarging Lesion Volume-EDSS	$R^2 = 0.05, p < 0.001$	—

NBV normalized brain volume, *NTV* normalized thalamic volume, *GMV* normalized gray matter volume, *PBVC* annualized percent brain volume change, *EDSS* expanded disability status scale

DISCUSSION

We demonstrate superior performance of the fully automatic, deep learning-based tool, iQ-MS, for detection of new, enlarging and contrast-enhancing lesions, the principal indicators of subclinical MS disease activity, compared with qualitative radiology reporting. We also show at least equivalent performance of the AI tool with semi-automated quantitative lesion activity and volumetric assessments undertaken by an experienced, ISO-9001 certified core imaging laboratory.

The detection of clinically silent new MRI lesions is an important determinant of treatment strategy⁵ that may, in its own right, lead to escalation of immunotherapy. Most modern therapeutic paradigms target No Evidence of Disease Activity (NEDA)⁸, which encompasses both clinical and radiological disease quiescence. Here, we report a case-level sensitivity of 93.3%, relative to a consensus ground truth, for detecting MS disease activity in multi-center, real-world MRI scans acquired ~12 months apart, an interval consistent with recommended routine clinical practice for monitoring MS and treatment efficacy. For this metric, the fully automatic AI based tool substantially outperformed clinical radiology reports (sensitivity 58.3%), despite only a minor sacrifice in specificity (97.6% vs 98.8%); and was at least equivalent to the

core imaging laboratory (sensitivity 91.7% in longitudinally consistent scans for both methods). Not surprisingly, when a subset of scans reported by fellowship-trained neuroradiologists was analyzed, the sensitivity of radiology reports for MS disease activity rose substantially (77%), but remained essentially stable at 92.3% for iQ-MS (data not shown).

At the lesion level, iQ-Solutions missed the equivalent of only 1 new lesion for every 44 scans analyzed in our cohort, whereas conventional radiology reports and the core lab missed the equivalent of 1 new lesion in 15 and 19 scans respectively. Using the average new lesion volume calculated by the AI tool and an approximation of the number of axons transected per mm³ of new lesional tissue²³, the application of iQ-MS therefore represents a potential opportunity to prevent, with appropriate treatment change, an averaged irreversible loss of >45,000 (up to >2 million in individual patients) axons, over 12 months relative to individuals monitored with conventional radiology reporting alone. These numerical extrapolations assume the availability of a therapy that can effectively prevent new lesion formation.

However, improved sensitivity for interval disease activity relative to radiology reports was driven primarily by failure of the human reporter to capture enlarging lesions consistently, perhaps not an unexpected finding given their visual subtlety in comparison with new, free-standing lesions. Enlarging lesions are under increasing scrutiny as a primary driver of disability worsening, especially for patients in whom relapses have been essentially abolished by high-efficacy DMT. In particular, slowly enlarging lesions, likely an imaging surrogate of “smoldering” MS lesions that exhibit chronic inflammation at their edge²⁴, have gained traction as an independent biomarker of disease progression with a distinct pathophysiology²⁵. Currently, iQ-MS does not isolate concentrically enlarging lesions from the global enlarging lesion pool, nor does it automatically monitor individual lesions over multiple timepoints to separate subacute from slow lesion enlargement. Incorporating these capabilities into AI-based lesion activity tools such as iQ-MS will become more pressing as pharmacotherapies that putatively target these pathomechanisms, such as the BTKi drugs, are developed²⁶.

The detection of contrast enhancement, a marker of blood-brain barrier disruption that characterizes new MS lesion formation and typically persists for 2–6 weeks, was also assessed in the 180 study scans in which gadolinium contrast was administered. While the sensitivity of iQ-MS for this metric (85.7%) was less impressive than for new and enlarging lesions, the fully automatic AI-based tool significantly outperformed (Table 4) the other methods with only a minor impact on specificity (97.2%). The omission of gadolinium administration from routine MS monitoring protocols^{27,28} further emphasizes the need for tools that sensitively detect interval development of new and enlarging lesions.

Accelerated brain atrophy occurs at the earliest stages of MS and is a recognized marker of neurodegeneration²⁹. The role of brain volumetrics in the clinical management of individual people with MS is less well defined. At the group level, there is good evidence that lower cross-sectional normalized brain volumes correlate with worse disability outcomes³⁰; and that short term (1–2 years) brain atrophy can predict longer term clinical outcomes³¹. Translation to individual patients is confounded by measurement error inherent to analysis techniques; longitudinal scan acquisition inconsistency; and biological and treatment-related fluctuations in brain volume³². However, brain volume below the 10th centile of an age-matched healthy control, a consistent adverse brain atrophy trajectory over multiple clinical epochs or severe PBVC (>0.8% per annum) over a single epoch, may influence or support changes in immunotherapy in conjunction with relevant clinical and lesion metrics. The current literature lacks clinical evaluation and validation data for existing quantitative volumetric reports for people with MS¹⁵.

Here, we report high correlations between the outputs of the AI tool and both cross-sectional and longitudinal whole brain volumetric tools measured in a core MRI lab using SIENAX³² ($R^2 = 0.67$) and SIENA³³ ($R^2 = 0.86$) respectively; and comparatively improved correlations with the EDSS (Table 6). Severe brain volume loss (<10th healthy control centile) was present in substantial proportion of study scans, but cross-sectional brain volume loss of any severity was only mentioned in a small proportion (<25%) of radiology reports, potentially reflecting assumed lack of clinical relevance of this metric by the reporting radiologist or inability of the human reporter to assess brain volume loss, even qualitatively, relative to a hypothetical, age-matched healthy control. Despite excellent correlation between the tools, there was a general tendency for NBV derived by the Core Lab's implementation of SIENAX to yield NBVs of lower centiles (referenced to the HC cohort) than iQ-MS (Table 5). In the absence of a true ground truth for brain volume measurement, the significance of this "shift" is uncertain, noting that iQMS-derived NBV did show improved (albeit modest) correlation with clinical outcomes (Table 6). The principal measure of clinical interest, annualized PBVC, was similar across the two quantitative tools (iQ-MS mean PBVC -0.32% , SIENA mean PBVC -0.36%), and fell within the range (<0.4% loss) considered non-pathological²². This is unsurprising in a modern MS cohort, given that many of the highly effective therapies, use of which is prevalent in Australia, ameliorate brain volume loss in randomized clinical trials^{34–36}. When stratified by severity, the tools appear to show equivalent interval PBVC among the atrophy subgroups when referenced to the same healthy control cohort analyzed with the respective methods (Table 5). However, the presence of severe atrophy (>0.8% negative PBVC), as determined by the two quantitative methods, was discordant in 24/295 (8.1%) of cases, highlighting methodological concerns when applying these tools to individual patients over single, relatively short epochs. Compared to SIENA, we have recently shown that DeepBVC, the brain atrophy algorithm embedded in iQ-MS, demonstrates greater stability and superior performance in test–retest experiments; and is more robust to variance in imaging acquisition¹⁹. Likely reflecting the inability of the human reporter to detect minor brain volume changes over short intervals, no interval atrophy was reported in any of the 236/295 scan pairs that were visually assessed.

When a clinician evaluates brain imaging in a person with MS, they mentally compare the scan before them not only with a hypothetical healthy person of similar age, but also with a hypothetical patient, derived from their cumulative experience, of similar age, disease duration and treatment. In conventional monitoring paradigms, such a comparison is necessarily indirect, qualitative and limited by the experience of the reporting radiologist and clinician. Existing quantitative imaging tools partly address this through comparison of individual patients to healthy controls, as does the fully automatic, AI tool described here. To our knowledge, this is the first tool to additionally embed an 'experiential' comparator that returns a relevant patient centile for both FLAIR lesion burden and brain volumetric data. While the clinical utility of this additional information is unknown, the integration of iQ-MS into the recently inaugurated MSBase Imaging Repository will facilitate the development of a broader comparative experiential dataset that can be properly benchmarked in research settings.

Finally, incidental findings (Table 2) were reported by the radiologist in 10.6% of MS scans. We emphasize that iQ-Solutions™ is a non-diagnostic tool designed for the quantitative monitoring of people with a known neurological disease, here applied to MS, to facilitate their precision treatment. Radiologist oversight, both for quality control of the results provided by the AI tool; and for reporting clinically significant incidental findings, remains paramount.

Our study has a number of limitations. The bulk of MRI scans in the study were acquired on one of three scanners, potentially

limiting the generalizability of the results. Additionally, most scan pairs (318/397) analyzed in our cohort were acquired on the same scanner with a consistent imaging protocol, as determined by iQ-MS, that may be difficult to enforce in some clinical settings. Although not a principal outcome of our study, the high correlation between cross-sectional lesion number/volume as determined by iQ-MS and the core lab should be interpreted with caution, given that image analysts in the core lab manually adjusted lesion masks that were initially created with an in-house AI algorithm that shared training data with the fully automatic solution. However, longitudinal lesion metrics (new and enlarging lesions), the outcome of most clinical relevance, were manually determined by the core lab via the aid of an independent subtraction image and slice by slice visual inspection. While the determination of the expert consensus was potentially confounded by lack of blinding (imposed by the distinct formats of the segmentations reviewed by the expert neurologist and neuroradiologist), the consensus was corroborated by an independent radiologist in all case-level discrepant scan pairs reviewed. Volumetric performance of the AI tool was confined to scan pairs with an available quantitative comparator. However, normalized brain volume and PBVC correlated strongly with de-facto gold standards used in the majority of modern MS clinical trials, exhibited less variance than these comparators, and better, though still weakly, correlated with a measure of clinical disability.

iQ-MS is a sensitive and accurate tool for monitoring MRI scans in people with MS by providing quantitative metrics that value-add to traditional radiology reports. Comparison with both radiology reports and a core MRI analysis lab shows superiority of the AI tool across a range of lesion and volume measures derived from clinically acquired, multicentre scans. The incorporation of an experiential patient reference provides a more clinically meaningful quantitative comparator for lesion burden and brain volumetric analyses. The scaled deployment of AI-based quantitative imaging tools, such as iQ-MS, has the potential to enhance both real-world, clinical-imaging disease-specific research and the precision management of individual patients with MS.

METHODS

Patients and clinical data

Patients with a diagnosis of MS attending the Royal Prince Alfred Hospital MS Service were retrospectively included in the study. The study was approved by The University of Sydney Human Research Ethics Committee and followed the tenets of the Declaration of Helsinki. Written informed consent was obtained from all participants. De-identified clinical data, including diagnosis, disease duration (from symptom onset), gender, age in years and expanded disability status scale (EDSS) score, were extracted through the clinic's MSBase³⁷ interface.

Imaging data and informatics

Inclusion criteria included a minimum of two available MRI timepoints, separated by at least 6 months. Scans with 3D T1-w and 3D FLAIR imaging, acquired on any MRI scanner, were included in the study; there were no pre-specified sequence parameters. Based on a significance level of 5%, assumed 80% sensitivity of radiologist reports for detection of MS lesion activity, and power of 80% to identify a 10% improvement with iQ-MS, recruitment to the study ended when 400 appropriate scan pairs had been included. All images were automatically de-identified with an informatics tool, Torana™ (Sydney Neuroimaging Analysis Centre, Sydney), prior to their inclusion in an in-house research PACS for automatic analysis and processing by iQ-MS. The MSBase identifier was automatically added to the image meta-data to facilitate subsequent matching with the patient's clinical data. To simulate real-time clinical workflow, annotations and reports

generated by iQ-Solutions were automatically returned to Torana™ and transferred into the appropriate project/subject/scan session in the PACS for review by study staff.

Clinical radiology reports

Clinical radiology reports were de-identified and then reviewed by an expert MS neurologist (MB), who extracted and recorded the following metrics: number of new FLAIR lesions, enlarging FLAIR lesions and T1-w CELs. Scans were categorized as active if any new/enlarging or enhancing lesions were detected. The burden of cerebral FLAIR MS pathology, where reported, was recorded and an attempt made to transform descriptors into a numerical rating made (Table 3). The presence/absence of reported brain volume loss and its severity (mild, moderate, severe) was recorded, as was the presence/absence of brain atrophy between current and prior studies. Incidental findings and their type were recorded. Reports were also categorized by whether the reporting radiologist was a fellowship-trained subspecialty neuro-radiologist or a general radiologist.

Core MRI reading laboratory

All scans were independently (and blindly) analyzed by trained neuroimaging analysis staff at the Sydney Neuroimaging Analysis Centre, an ISO-9001 certified and CFR-21 Part 11-compliant core MRI reading facility, using standard operating procedures (SOP) designed for regulatory MS clinical trials. Expert human QA was undertaken at multiple steps for each of the following analysis pipelines. FLAIR lesion number and volume were iteratively measured on intensity-inhomogeneity corrected 3D FLAIR imaging using an in-house lesion segmentation tool, followed by manual quality control of every image slice and lesion mask adjustment with a semi-automated thresholding technique. Importantly, the in-house tool for measurement of these (cross-sectional) lesion metrics used an AI algorithm that shared training data with the fully automatic solution used by iQ-MS. Lesion activity analysis (the development of new or enlarging lesions) was performed manually with the aid of a subtraction image and slice-by-slice inspection. Enlarging lesions were defined as any pre-existing FLAIR hyper-intensity that had enlarged, either concentrically or eccentrically, between the prior and current scan on ≥ 2 consecutive slices. Scans were categorized as active if any new/enlarging or enhancing lesions were detected. CELs were identified on co-registered post contrast 3DT1 images and enhancing voxels segmented using a semi-automated thresholding technique.

Quality control determined by the core lab's SOP for observational studies was implemented to exclude scans unsuitable for cross-sectional or longitudinal analysis (Supplementary methods). At each time point, the quantification of absolute and NBV and thalamus volume was estimated on co-registered pre-contrast lesion in-painted and inhomogeneity-corrected 3D T1-w images using FMRIB's SIENAX (version 2.6)³³ and FIRST³⁸ software packages respectively. Quantification of longitudinal PBVC between the current and prior scan was determined by a modified hybrid of FMRIB's SIENA³³ software. Annualized brain atrophy was categorized as normal ($<0.4\%$), mild-moderate ($0.4\text{--}0.8\%$) or severe ($>0.8\%$).

iQ-Solutions™ MS report

All iQ-MS data was derived automatically using the workflow described under Imaging Data and Informatics above; for clarity, no human intervention was introduced at any point. Specific metrics returned by iQ-MS are shown in Table 1. FLAIR MS lesion burden was categorized using the automatically returned patient (MS population) centile figure (see Introduction, Table 3) as mild (<25 th patient centile), moderate (25th–75th patient centile) or severe (>75 th patient centile). Brain volume loss was categorized using the automatically returned HC centile figure (Table 3) as none (≥ 25 th HC centile), mild-moderate (10–25th HC centile) or

severe (≤ 10 th HC centile). Annualized brain atrophy was categorized as normal ($\leq 0.4\%$), mild-moderate ($>0.4\%$, $\leq 0.8\%$) or severe ($>0.8\%$), based on previously determined 'pathological cut-offs' of brain atrophy using SIENA²², against which the relevant iQ-MS algorithm has been previously validated¹⁹.

Expert consensus

To establish a ground truth, a case and lesion level comparison of the output of each method (radiology report, neuroimaging analyst, iQ-MS) was undertaken. Where there was agreement at both the case (active vs inactive) and lesion (number of new lesions, enlarging lesions and CELs) level across all three methods, the results were accepted as the ground truth. Where any discrepancy was noted at either the case or the lesion level, further review of the raw images, together with the output of all three methods (including final segmentations from both neuroimaging analysts and iQ-MS) was undertaken by an expert neuro-radiologist (YB) and neurologist (MB) and a final ground truth established by consensus. As the segmentation masks output by the three methods differed in both format and visual appearance, this review was necessarily unblinded. As such, a random sample of $>25\%$ of all case-level discrepant scan results was reviewed by a third, independent expert neuroradiologist to determine conformity with the expert consensus.

Statistics

Statistical analyses were performed using SPSS 26.0 (SPSS, Chicago, IL, USA). Descriptive statistics were calculated for all inter-method comparisons. Subgroups studied included (i) scans reported by a subspecialist neuroradiologist and (ii) scan pairs acquired with a longitudinally consistent imaging protocol as defined in Supplementary methods. Unless otherwise described in the result, Pearson's correlation coefficient was used to measure statistical dependence between two numerical arrays, and $p < 0.05$ was considered statistically significant. For partial correlation, data were adjusted for age, gender and disease duration; $p < 0.05$ was considered statistically significant.

Reporting summary

Further information on research design is available in the Nature Research Reporting Summary linked to this article.

DATA AVAILABILITY

The datasets analyzed in the current study are available from the corresponding author on reasonable request and with a relevant research agreement.

CODE AVAILABILITY

The underlying code for iQ-Solutions™ is not publicly available for proprietary reasons; however, code for specific individual algorithms is described in the relevant refs.^{17–19}.

Received: 20 July 2023; Accepted: 29 September 2023;

Published online: 19 October 2023

REFERENCES

- Walton, C. et al. Rising prevalence of multiple sclerosis worldwide: Insights from the Atlas of MS, third edition. *Mult. Scler.* **26**, 1816–1821 (2020).
- Cree, B. A. C. et al. Silent progression in disease activity-free relapsing multiple sclerosis. *Ann. Neurol.* **85**, 653–666 (2019).
- Kappos, L. et al. Contribution of relapse-independent progression vs relapse-associated worsening to overall confirmed disability accumulation in typical relapsing multiple sclerosis in a pooled analysis of 2 randomized clinical trials. *JAMA Neurol.* **77**, 1132–1140 (2020).

4. Sharrad, D., Chugh, P., Slee, M. & Bacchi, S. Defining progression independent of relapse activity (PIRA) in adult patients with relapsing multiple sclerosis: a systematic review. *Mult. Scler. Relat. Disord.* **78**, 104899 (2023).
5. Barnett, M., Barnett, Y. & Reddel, S. MRI and laboratory monitoring of disease-modifying therapy efficacy and risks. *Curr. Opin. Neurol.* **35**, 278–285 (2022).
6. Cagol, A. et al. Association of brain atrophy with disease progression independent of relapse activity in patients with relapsing multiple sclerosis. *JAMA Neurol.* **79**, 682–692 (2022).
7. De Stefano, N. et al. Assessing brain atrophy rates in a large population of untreated multiple sclerosis subtypes. *Neurology* **74**, 1868–1876 (2010).
8. Lu, G. et al. The evolution of “No Evidence of Disease Activity” in multiple sclerosis. *Mult. Scler. Relat. Disord.* **20**, 231–238 (2018).
9. Ross, D. E., Ochs, A. L., DeSmit, M. E., Seabaugh, J. M. & Havranek, M. D., Alzheimer’s Disease Neuroimaging I. Man versus machine Part 2: comparison of radiologists’ interpretations and NeuroQuant measures of brain asymmetry and progressive atrophy in patients with traumatic brain injury. *J. Neuropsychiatry Clin. Neurosci.* **27**, 147–152 (2015).
10. Ross, D. E., Ochs, A. L., Seabaugh, J. M. & Shrader, C. R., Alzheimer’s Disease Neuroimaging I. Man versus machine: comparison of radiologists’ interpretations and NeuroQuant(R) volumetric analyses of brain MRIs in patients with traumatic brain injury. *J. Neuropsychiatry Clin. Neurosci.* **25**, 32–39 (2013).
11. Dwyer, M. G. et al. Salient central lesion volume: a standardized novel fully automated proxy for brain FLAIR lesion volume in multiple sclerosis. *J. Neuroimaging* **29**, 615–623 (2019).
12. Kamraoui, R. A. et al. DeepLesionBrain: towards a broader deep-learning generalization for multiple sclerosis lesion segmentation. *Med. Image Anal.* **76**, 102312 (2022).
13. Ma, Y. et al. Multiple sclerosis lesion analysis in brain magnetic resonance images: techniques and clinical applications. *IEEE J. Biomed. Health Inf.* **26**, 2680–2692 (2022).
14. Rovira, A. et al. Assessment of automatic decision-support systems for detecting active T2 lesions in multiple sclerosis patients. *Mult. Scler.* **28**, 1209–1218 (2022).
15. Mendelsohn, Z. et al. Commercial volumetric MRI reporting tools in multiple sclerosis: a systematic review of the evidence. *Neuroradiology* **65**, 5–24 (2023).
16. Çiçek, Ö, Abdulkadir, A., Lienkamp, S. S., Brox, T., Ronneberger, O. 3D U-Net: learning dense volumetric segmentation from sparse annotation. In *Proc. International Conference on Medical Image Computing and Computer-Assisted Intervention*: 2016.
17. Cabezas, ML, Y., Kyle, K., Ly, L., Wang, C., Barnett, M. Estimating lesion activity through feature similarity: a dual path Unet approach for the MSSEG2 MICCAI challenge. In *Proc. 2nd MICCAI Challenge on Multiple Sclerosis New Lesions Segmentation Challenge Using a Data Management and Processing Infrastructure. MICCAI-MSSEG-2*. Edited by Commowick FC, F.; Cotton, F.; Dojat, M. 107–110 (2021).
18. Tang, Z. et al. LG-Net: lesion gate network for multiple sclerosis lesion inpainting. In: de Bruijne, M. et al. *Medical Image Computing and Computer Assisted Intervention—MICCAI 2021. Lecture Notes in Computer Science*, vol 12907. https://doi.org/10.1007/978-3-030-87234-2_62 (Springer, Cham, 2021).
19. Zhan, G. et al. Learning from pseudo-labels: deep networks improve consistency in longitudinal brain volume estimation. *Front. Neurosci.* **17**, 1196087 (2023).
20. Nakamura, K. et al. Jacobian integration method increases the statistical power to measure grey matter atrophy in multiple sclerosis. *Neuroimage Clin.* **4**, 10–17 (2014).
21. Minagar, A. et al. The thalamus and multiple sclerosis: modern views on pathologic, imaging, and clinical aspects. *Neurology* **80**, 210–219 (2013).
22. De Stefano, N. et al. Establishing pathological cut-offs of brain atrophy rates in multiple sclerosis. *J. Neurol. Neurosurg. Psychiatry* **87**, 93–99 (2016).
23. Trapp, B. D. et al. Axonal transection in the lesions of multiple sclerosis. *N. Engl. J. Med.* **338**, 278–285 (1998).
24. Prineas, J. W. et al. Immunopathology of secondary-progressive multiple sclerosis. *Ann. Neurol.* **50**, 646–657 (2001).
25. Klistorner, S. et al. Expansion of chronic lesions is linked to disease progression in relapsing-remitting multiple sclerosis patients. *Mult. Scler.* **27**, 1533–1542 (2021).
26. Kramer, J., Bar-Or, A., Turner, T. J. & Wiendl, H. Bruton tyrosine kinase inhibitors for multiple sclerosis. *Nat. Rev. Neurol.* **19**, 289–304 (2023).
27. Brisset, J. C. et al. New OFSEP recommendations for MRI assessment of multiple sclerosis patients: special consideration for gadolinium deposition and frequent acquisitions. *J. Neuroradiol.* **47**, 250–258 (2020).
28. Wattjes, M. P. et al. 2021 MAGNIMS-CMSC-NAIMS consensus recommendations on the use of MRI in patients with multiple sclerosis. *Lancet Neurol.* **20**, 653–670 (2021).
29. Calabrese, M. et al. Cortical atrophy is relevant in multiple sclerosis at clinical onset. *J. Neurol.* **254**, 1212–1220 (2007).
30. Giorgio, A. & De Stefano, N. Effective utilization of MRI in the diagnosis and management of multiple sclerosis. *Neurol. Clin.* **36**, 27–34 (2018).
31. Popescu, V. et al. Brain atrophy and lesion load predict long term disability in multiple sclerosis. *J. Neurol. Neurosurg. Psychiatry* **84**, 1082–1091 (2013).
32. Beadnall, H. N. et al. Comparing longitudinal brain atrophy measurement techniques in a real-world multiple sclerosis clinical practice cohort: towards clinical integration? *Ther. Adv. Neurol. Disord.* **12**, 1756286418823462 (2019).
33. Smith, S. M. et al. Accurate, robust, and automated longitudinal and cross-sectional brain change analysis. *Neuroimage* **17**, 479–489 (2002).
34. De Stefano, N., Silva, D. G. & Barnett, M. H. Effect of Fingolimod on brain volume loss in patients with multiple sclerosis. *CNS Drugs* **31**, 289–305 (2017).
35. Coles, A. J. et al. Alemtuzumab CARE-MS II 5-year follow-up: efficacy and safety findings. *Neurology* **89**, 1117–1126 (2017).
36. Kolind, S. et al. Ocrelizumab-treated patients with relapsing multiple sclerosis show volume loss rates similar to healthy aging. *Mult. Scler.* **29**, 741–747 (2023).
37. Butzkueven, H. et al. MSBase: an international, online registry and platform for collaborative outcomes research in multiple sclerosis. *Mult. Scler.* **12**, 769–774 (2006).
38. Patenaude, B., Smith, S. M., Kennedy, D. N. & Jenkinson, M. A Bayesian model of shape and appearance for subcortical brain segmentation. *Neuroimage* **56**, 907–922 (2011).

ACKNOWLEDGEMENTS

The authors would like to acknowledge funding support from Australian Government Department of Industry (CRCPFIVE000141). C.W. would like to acknowledge the support from the Nerve Research Foundation at The University of Sydney and Multiple Sclerosis Australia (18–0461).

AUTHOR CONTRIBUTIONS

M.B., D.W., Y.B. and C.W. conceived the study and planned the experiments; M.B., H.B., K.K., L.L., L.M., Y.B. contributed to data preparation. D.W. and A.S. led the Core Technology data analysis. M.B., H.B. and L.M. contributed to clinical report interpretation and data extraction; L.L. and K.K. led core MRI reading center data analysis; M.B. and C.W. carried out the statistical analysis. M.B., D.W., Y.B. and C.W. wrote the initial draft of the manuscript. M.B. and D.W. were considered co-first authors and contributed equally. Y.B. and C.W. were considered co-senior authors and contributed equally. All authors provided critical feedback and intellectual input throughout the study, revised the initial draft, and contributed to the final version, of the submitted manuscript.

COMPETING INTERESTS

The authors declare the following financial/non-financial competing interests: D.W., K.K., L.L., A.S., Z.T., G.Z. and C.W. are employees of Sydney Neuroimaging Analysis Centre (SNAC); M.B. is a consulting neurologist and director for research at SNAC; T.D. and Y.B. are consulting radiologists at SNAC. C.W. and Y.B. personally hold equity ownership in SNAC, the entity that manufactures iQ-Solutions™

ADDITIONAL INFORMATION

Supplementary information The online version contains supplementary material available at <https://doi.org/10.1038/s41746-023-00940-6>.

Correspondence and requests for materials should be addressed to Chenyu Wang.

Reprints and permission information is available at <http://www.nature.com/reprints>

Publisher’s note Springer Nature remains neutral with regard to jurisdictional claims in published maps and institutional affiliations.



Open Access This article is licensed under a Creative Commons Attribution 4.0 International License, which permits use, sharing, adaptation, distribution and reproduction in any medium or format, as long as you give appropriate credit to the original author(s) and the source, provide a link to the Creative Commons license, and indicate if changes were made. The images or other third party material in this article are included in the article’s Creative Commons license, unless indicated otherwise in a credit line to the material. If material is not included in the article’s Creative Commons license and your intended use is not permitted by statutory regulation or exceeds the permitted use, you will need to obtain permission directly from the copyright holder. To view a copy of this license, visit <http://creativecommons.org/licenses/by/4.0/>.

© The Author(s) 2023